

EUROPEAN ORGANIZATION FOR NUCLEAR RESEARCH

Proposal to the ISOLDE and Neutron Time-of-Flight Committee

Development of new rare-earth-free hard magnetic materials

[May 13, 2020]

D. Zيابkin¹, I. Unzueta², R. Mantovan³, H. P. Gunnlaugsson⁴, H. Masenda⁵, D. Naidoo⁵, K. Bharuth-Ram⁶, J. Schell^{7,8}, P. B. Krastev⁹, S. Ólafsson¹⁰, B. Qi¹⁰, T. T. Dang⁷, K. Johnston⁸, D. C. Lupascu⁷, P. Schaaf¹

¹Department of Materials for Electronics, Institute of Materials Science and Engineering, TU Ilmenau, Gustav-Kirchhoff-Strasse 5, 98693 Ilmenau, Germany

²Department of Applied Mathematics, University of the Basque Country UPV/EHU, 48013 Bilbao, Spain

³Laboratorio MDM, IMM-CNR, Via Olivetti 2, 20864, Agrate Brianza (MB), Italy

⁴Science Institute, University of Iceland, Dunhaga 3, IS-107 Reykjavík, Iceland

⁵School of Physics, University of the Witwatersrand, WITS 2050, South Africa

⁶University of KwaZulu-Natal, Durban 4001, South Africa

⁷Institute for Materials Science and Center for Nanointegration Duisburg-Essen (CENIDE), University of Duisburg-Essen, 45141 Essen, Germany

⁸European Organization for Nuclear Research (CERN), CH-1211 Geneva, Switzerland

⁹Institute for Nuclear Research and Nuclear Energy, Bulgarian Academy of Sciences, 72 Tsarigradsko Chaussee Boulevard, Sofia, 1784, Bulgaria

¹⁰Science Institute, University of Iceland, 107, Iceland

Spokesperson(s): Dmitry Zيابkin (dmitry.zyabkin@tu-ilmenau.de) & Peter Schaaf (peter.schaaf@tu-ilmenau.de)

Local contact: Juliana Schell (juliana.schell@cern.ch), Karl Johnston (karl.johnston@cern.ch)

Abstract

Mn-based compounds possess numerous attractive properties, which are of interest from both fundamental physics point of view and particularly attractive for different applications in modern technology, from magnetic storage to sensing and spin-based electronics. The possibility to adjust and finely tune their magnetic properties through stoichiometry engineering is highly important in order to target different applications. In this project, the Mössbauer effect will be applied on ⁵⁷Fe/Sn sites following implantation of radioactive ⁵⁷Mn and ¹¹⁹In to probe the micro-structure and magnetism of Mn-based alloys at the atomic-scale. Here we propose the experimental plan which aims at establishing of a direct correlation between the local structure and bulk magnetism (and other physical properties) of Mn-based alloys.

Requested shifts: 15 shifts, (split into ~ 3 runs over ~ 3 years)



1 INTRODUCTION/MOTIVATION

In modern society, minimising carbon emission has clearly become of paramount importance. This benefits from the development of new highly efficient autonomous electric vehicles, increasing power saving in electronics, boosting clean energy generation and various other projects. The majority of these applications, such as electrical mechanisms, power supply units or other devices that require electromagnetic conversion rely firmly on the hard-magnetic materials. These materials possess large hysteresis as well as saturation magnetization and, in the scenarios where high performance is needed, they are based on rare-earth (RE) metals ($\text{Nd}_2\text{Fe}_{14}\text{B}$). Successful production of such materials depends on the availability of RE, especially Nd, Dy and Tb, demand for which has been constantly growing. Employment of the RE metals allows one to preserve magnetic properties up to ≈ 500 K. However, the maximum energy product has not shown improvement of properties in the past 20 years for the bulk magnetic materials. Doubtless, further development of RE based hard-magnets becomes hardly feasible, whilst both available materials and new methods of their production are absent (1, 2). An attractive alternative is hard magnets of MnGa (Al, Bi) compounds, which have been the subject of recent studies (1, 3) and which may fill the niche in the maximum energy product between hard ferrite magnets (<5 MGOe) and RE magnets (>30 MGOe).

Presently, promising candidates for this application are certain $L1_0$ ordered binary manganese compounds. Although Mn alone is antiferromagnetic, when it is alloyed with other elements it becomes a strong ferromagnet (4). In our study we propose to investigate three Mn-based systems and study both their underlying structure and their magnetic properties. As the main tool for such studies, we propose to employ $^{57}\text{Mn}/\text{Fe}$ ($T_{1/2} = 1.5$ min) and $^{119}\text{In}/\text{Sn}$ ($T_{1/2} = 2.4$ min) emission Mössbauer spectroscopy (eMS).

1.1 MnAl compounds

$L1_0$ MnAl is a system with tetragonal structure, which has interesting magnetic properties demonstrating saturation magnetization $M_s > 0.7$ MA/m, magnetic anisotropy $K_1 > 1.5$ MJ/m³ and Curie temperature $T_c > 600$ K (5). The presence of ferromagnetic exchange between Mn-Mn atoms is an interesting feature of this system and contradicts the antiferromagnetic trend in half-filled bands. These features make this class of compounds of broad interest. The $L1_0$ structure (or τ -phase) is the only ferromagnetic phase in the MnAl system. As it seems, one may need to obtain equatomic and well-ordered Mn₅₀Al₅₀ composition, where Mn atoms occupy 1a (0, 0, 0) sites and induce ferromagnetism, whilst Al atoms sit at the 1d (1/2, 1/2, 1/2) sites and have tiny magnetic moment to achieve the highest magnetic output.

The $L1_0$ phase, however, exists only when the condition $\text{Mn}_{50+x}\text{Al}_{50-x}$ ($1 \leq x \leq 8$) is satisfied. Unfortunately, due to the nature of Mn, the surplus Mn atoms enter 1d (1/2, 1/2, 1/2) sites and start to act antiferromagnetically with the Mn atoms at 1a (0, 0, 0) sites (6). Despite various alterations in Mn/Al ratios, the $L1_0$ structure is metastable and decomposes into two non-magnetic phases (β -Mn and γ_2) (7). Doping with ions has been attempted to overcome this drawback, with the highest attention paid to interstitial (carbon) and substitutional doping (3d elements). Despite the positive impact on the phase stability, the intrinsic magnetic properties after doping, such as the Curie temperature and magnetic anisotropy, often deteriorate (8). As most of the time the desired τ -phase forms in a heterogeneous way (at remnants of the ϵ -phase) close attention need to be paid to the phase evolution dynamics (see Fig.1).

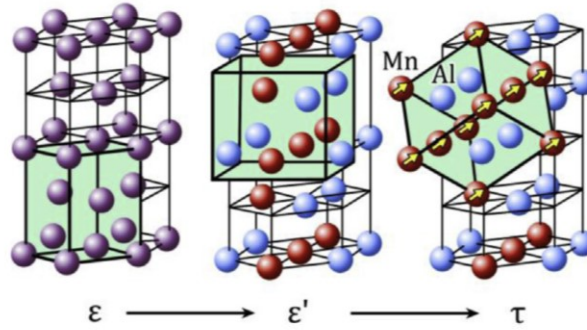


Fig.1. MnAl alloy phase formation. The ferromagnetic t structure forms through different Mechanisms (1).

A handful of studies exist, which suggests that alloying with 3d metals of atomic radii close to those of Al or Mn (i.e. substitutional doping) and having fewer valence electrons may be beneficial for improving the $L1_0$ phase stability and saturation magnetization (8). At present, there is a lack of systematic investigation of how the substitutional dopants affect the magnetic properties, and consequently there is no clear understanding in which direction one may go in order to both preserve the phase and improve the intrinsic magnetism. Hence, our proposal employs the extreme sensitivity of $^{57}\text{Mn}/\text{Fe}$ emission Mössbauer spectroscopy to elucidate the evolution of the internal magnetic field at the atomic scale during phase formations and their thermal behaviour as well as the role of defects (twins mainly) on the observed magnetic behaviour.

Presently, one may expect that implanted ^{57}Mn atoms occupy Mn sites and further decay into Fe. The desired condition of having fewer valence electrons and similar atom radius can be easily satisfied. Another advantage of using eMS experiments is due to the dilute concentrations of probe atoms ($\leq 10^{-4}$ at. %), there is unlikely an exchange interaction among the probe atoms. This fact allows one not to disturb the local environment much. A combination of eMS studies with theoretical calculations is strongly desired in order to establish the criteria for further refinement of the magnetic properties of this promising material.

1.2 MnBi compounds

Another promising alternative to MnAl compounds, especially for application at elevated temperatures, with a higher maximum energy product is MnBi (9). Among several possible phases only the low temperature phase (LTP) is of primary interest. This phase is ferromagnetic (shown in Fig.2., disordered hexagonal NiAs structure, $P63 / mmc$ symmetry) and remains this way until 628 K, after this it undergoes a transition to a paramagnetic high-temperature phase.

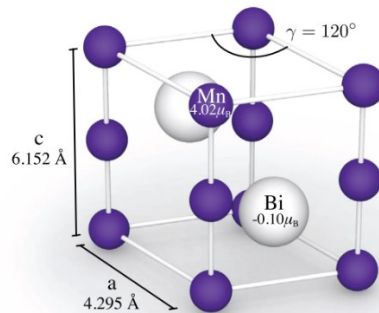


Fig.2. Structure of LTP (MmBi) (10).

This LTP goes through a spin-reorientation process with temperature ramping from 0 K (11)(12). When exposed to high temperature there is a peculiarity in the coercivity of the LTP which rises with temperature and is significantly larger than coercivity of the Nd–Fe–B magnets at elevated temperatures. Despite all advantages of the LTP it has not been produced as a single-phase material and the structure always includes segregation of Mn, thus hindering one from obtaining the maximum energy product possible. There are various pathways in order to improve it. One of the most promising ways is to take advantage of large magneto crystalline anisotropy of LTP by setting up an exchange coupling with a soft phase (Co, Fe) (13). Theory suggests that if that coupling is applied successfully, it may boost maximum energy product to as high as 40 MGOe (14). This strategy was observed to work in the case of MnAl compound as it was reported that doping with a small amount of transition metals can double the magnetization (15). Doping up to several at.%, however, was observed to have a generally harmful effect (16). Therefore, we propose to study the local environment of MnBi compounds doped with extremely low concentrations of $^{57}\text{Mn}/\text{Fe}$ atoms and track the development of magnetic structure as a function of temperature and magnetic fields. There is a strong desire to unveil changes at the interface of MnBi/X (Co, Fe, Ni) and to follow the diffusion.

1.3 MnGa compounds

MnGa compounds which contain neither rare earth nor noble metal atoms are promising candidates for high-density perpendicular magnetic recording (17, 18) as well as for novel permanent magnetic materials due to their high Curie temperature $T_c \approx 630$ K (19) and strong magnetic anisotropy field (20). The structure of Mn_xGa alloys is identical to that described for MnAl in section 1.2. Mn_xGa alloys exhibit a tetragonal ferromagnetic $L1_0$ phase in the $0.76 \leq x \leq 1.9$ composition range, whilst from $2 \leq x \leq 3$, the $L1_0$ structure turns

into a $D0_{22}$ structure (20). In the present proposal we will focus on the $L1_0$ phase. The magnetic contribution of Mn_xGa samples comes from the Mn atoms in which the d -electrons are highly localized, giving rise to large spin polarization within each Mn atom (21). However, the d -electrons have a strong itinerancy through the hybridization of p -orbitals of Ga atoms, which promotes the ferromagnetic arrangement of the magnetic moments (21). The role of Ga atoms in the magnetism of Mn_xGa alloys is considered as negligible.

In relation to the previous IS578 proposal, where eMS technique was applied to Mn_xGa samples, one may expect to observe large hyperfine fields while implanting $^{57}\text{Mn}/\text{Fe}$ ions (going substitutional on Mn sites), and almost negligible hyperfine fields by implanting $^{119}\text{In}/\text{Sn}$ ions (going substitutional on Ga sites). However, as Fig. 3 shows, during $^{119}\text{In}/\text{Sn}$ eMS measurements carried out at ISOLDE on a $\text{Mn}_{0.8}\text{Ga}$ sample, a strong angular dependence of the emission intensity was observed and, contrary to what was expected, huge hyperfine fields were recorded at Ga sites. The ^{119}Sn eMS study on the remaining Mn_xGa ($0.7 \leq x \leq 1.9$) samples could not be completed before the LS2.

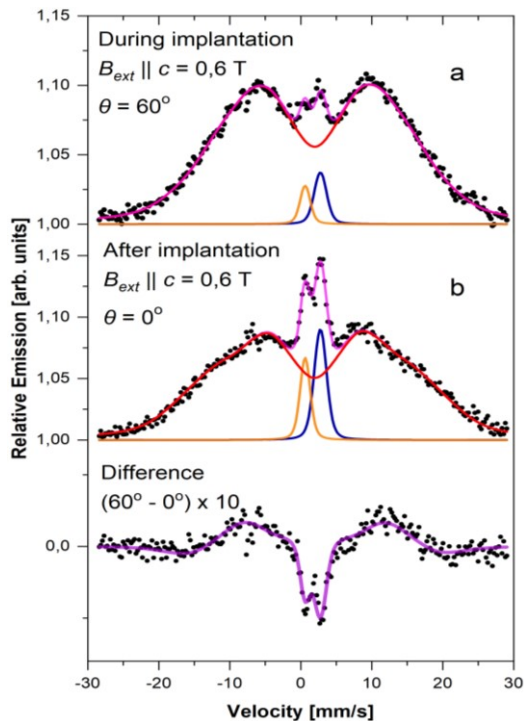


Fig.3. MnGa measured at angles of 60° and 0° under 0.6T during (a) and after (b) implantation. Angular dependence on the emission intensity of $^{119}\text{In}/\text{Sn}$ eMS measurements in $\text{Mn}_{0.8}\text{Ga}$ alloys. Huge hyperfine fields were recorded, indicating a clear magnetic nature of Ga sites.

The ISOLDE facility, in combination with the available eMS set-up, provides a unique tool to elucidate the origin of the observed angular dependence and the large hyperfine field at Ga sites in Mn_xGa samples, which is otherwise impossible using conventional Mössbauer spectroscopy. The main

objective of applying $^{57}\text{Mn}/\text{Fe}$ and $^{119}\text{In}/\text{Sn}$ eMS at ISOLDE is to determine the origin of the observed huge hyperfine fields and inquire into the cause of the strong eMS angular dependence observed. The envisaged results have the potential to enable a new explanation of the magnetic nature of these samples.

2. METHODS AND SAMPLES

In the current proposal we intend to use both ^{57}Mn and ^{119}In isotopes for emission Mössbauer spectroscopy to explore the magnetic properties of Mn-based rare-earth-free hard magnets. The method is well-known for the unambiguous determination the charge and spin state of the probe and allows one to determine the exact local environment of it (e.g. amorphous zones, layers or lattice sites). Performing the experiments with Mn isotope is an ideal scenario, since after the implantation Mn is expected to find itself on Mn sites in the host (no chemical difference - no additional impact). After it decays one gets an emission spectrum with relevant information such as charge and magnetic hyperfine field, both get affected by numerous factors taking place in the vicinity of the probe. The presence of electrically active defects nearby allows one to identify them and their configurations. On the other hand, ^{119}In isotopes are more sensitive to the magnetic hyperfine interactions. Another reason to employ eMS at ISOLDE lies in the fine concentration of the implanted probes. This means that the implanted atoms do not agglomerate nor interact with each other. Besides, it is of big interest to study the defect formation under ion implantation. Since Mn-based compounds tend to form twins relatively easily varying annealing one can study a possible nucleation mechanism and domain pinning strength at the twins (22). Hence, the eMS method, based on ion-implantation, is an ideal tool to study the role of defects in determining magnetic properties. Abilities to control the dose and utilizing dilute concentrations result in non-overlapping damage cascades that re-crystallizes at lower temperatures than amorphous layers, and in some cases (some metal systems) far below RT (23). Generally, Fe atoms in 4–5 different configurations can be well determined from eMS (depending on the complexity of the spectra), which is not possible with synchrotron Mössbauer methods.

After measurements performed using eMS, additional Mössbauer studies are going to be conducted at home laboratories (in Conversion Electron arrangement). The eMS collaboration at ISOLDE/CERN has in its possession a new eMS set-up (eMIL) (24), which allows to perform experiments in a broad temperature range and measurements can be done during implantation, time delayed and varying emission angles. For the full feasibility of the current proposal we have obtained funding to construct a set-up extension for eMIL – eMMA. The last is going to facilitate studies of magnetic materials and allow measurements in an external magnetic field up to 2.5 T. There is a high probability that a special sample holder will be constructed to perform cooling and heating in this 2.5 T field

For this proposal a series of MnAl samples with varying ratios [Mn_xAl ($x = 49, 52, 55, 58 \& 60$)] and various substrates (textured) will be produced by magnetron sputtering at TU Ilmenau. As produced samples are going to be studied by various conventional means including Vibrating Sample Magnetometer, X-ray diffractometry, different microscopy methods. A series of MnBi samples [Mn_xBi ($x = 49, 52, 55, 58 \& 60$)] including samples with the soft phase interface layers (Co) will be prepared by magnetron sputtering and electron beam methods. A series of samples prepared using Molecular Beam Epitaxy is additionally planned. Regarding the Mn_xGa samples ($L1_0$), five different Mn_xGa films ($L1_0$) have been selected: $\text{Ma}_{0.7}\text{Ga}$, $\text{Ma}_{0.8}\text{Ga}$, $\text{Ma}_{1.1}\text{Ga}$, $\text{Ma}_{1.4}\text{Ga}$ and $\text{Ma}_{1.9}\text{Ga}$. The wide range of composition is going to allow a systematic study of how the implantation affects the hyperfine fields (and therefore, magnetic properties) as well as the magnetic moments in Ga sites as a function of Mn content.

Summary of requested shifts:

Isotope	Minimum intensity/ μC	Beam energy	Shifts	Target	Ion Source
^{57}Mn (1.5 min)	$(2-3)\times 10^8$	≥ 40 keV	10	UC_x	Mn RILIS
^{119}In (2.1 min)	$(2-3)\times 10^8$	≥ 40 keV	5	UC_x	In RILIS

Table 1: Proposed beam request.

3 CONCLUSIONS/OUTLOOK

Performing experiments with dilute concentrations of dopant on possible new rare-earth-free hard magnetic materials is of huge importance and is strongly motivated by a shrinkage of supplies in the near future and global movement towards green energy. The raised questions in sections 1.1-1.3 can be answered when combined with additional information on the defect formation, phase transition, kinetics of defect annealing, electronic and magnetic properties of the Mn-based compounds and feasibility of low fluence implantation studies with the current systems.

References:

1. J. Cui *et al.*, *Acta Mater.* **158**, 118–137 (2018).
2. H. Nakamura, *Scr. Mater.* **154**, 273–276 (2018).
3. J. M. D. Coey, *J. Phys. Condens. Matter.* **26** (2014), doi:10.1088/0953-8984/26/6/064211.
4. T. Ohtani ; N. Kato ; S. Kojima ; K. Kojima ; Y. Sakamoto ; I. Konno ; M. Tsukahara ; T. Kubo, *IEEE Trans. Magn.* **M**, 1328–1330 (1977).
5. J. H. Park *et al.*, *J. Appl. Phys.* **107**, 1–4 (2010).
6. H. Kōno, Erratum: “On the Ferromagnetic Phase in Manganese-Aluminum System.” *J. Phys. Soc. Japan.* **14** (1959), pp. 237–237.
7. A. Edström, J. Chico, A. Jakobsson, A. Bergman, J. Ruzs, *Phys. Rev. B - Condens. Matter Mater. Phys.* **90**, 1–5 (2014).
8. S. Zhao *et al.*, *Phys. Rev. Appl.* **11**, 1 (2019).
9. V. N. Antonov, V. P. Antropov, *Low Temp. Phys.* **46**, 3–32 (2020).
10. J. Barker, O. Mryasov, *J. Phys. D. Appl. Phys.* **49** (2016), doi:10.1088/0022-3727/49/48/484002.
11. Y. B. Yang *et al.*, *J. Magn. Magn. Mater.* **330**, 106–110 (2013).
12. J. B. Yang *et al.*, *J. Appl. Phys.* **91**, 7866–7868 (2002).

13. T. R. Gao *et al.*, *Phys. Rev. B.* **94**, 2–6 (2016).
14. Y. Q. Li *et al.*, *IEEE Trans. Magn.* **393**, 484–489 (2013).
15. M. Matsumoto, A. Morisako, J. Ohshima, *J. Appl. Phys.* **69**, 5172–5174 (1991).
16. P. Kharel *et al.*, *J. Appl. Phys.* **111**, 1–4 (2012).
17. L. Zhu *et al.*, *Adv. Mater.* **24**, 4547–4551 (2012).
18. H. Kurt, K. Rode, M. Venkatesan, P. Stamenov, J. M. D. Coey, *Phys. Status Solidi Basic Res.* **248**, 2338–2344 (2011).
19. S. Mao *et al.*, *Sci. Rep.* **7**, 1–7 (2017).
20. Q. M. Lu *et al.*, *Sci. Rep.* **5**, 1–5 (2015).
21. A. Sakuma, *J. Magn. Magn. Mater.* **187**, 105–112 (1998).
22. S. Bance, F. Bittner, T. G. Woodcock, L. Schultz, T. Schrefl, *Acta Mater.* **131**, 48–56 (2017).
23. C. W. White *et al.*, *Nucl. Inst. Methods Phys. Res. B.* **7–8**, 473–478 (1985).
24. D. V. Zyabkin *et al.*, *Nucl. Instruments Methods Phys. Res. Sect. A.* **968**, 163973 (2020).

Appendix

DESCRIPTION OF THE PROPOSED EXPERIMENT

The experimental setup comprises: *(name the fixed-ISOLDE installations, as well as flexible elements of the experiment)*

Part of the Choose an item.	Availability	Design and manufacturing
SSP-GLM chamber	<input checked="" type="checkbox"/> Existing	<input checked="" type="checkbox"/> To be used without any modification
Mössbauer set-up (eMIL) and Mössbauer magnetic analyser (eMMA)	<input checked="" type="checkbox"/> Existing	<input checked="" type="checkbox"/> To be used without any modification <input type="checkbox"/> To be modified
	<input checked="" type="checkbox"/> New	<input type="checkbox"/> Standard equipment supplied by a manufacturer <input checked="" type="checkbox"/> CERN/collaboration responsible for the design and/or manufacturing
Existing equipment in the SSP lab in building 508	<input checked="" type="checkbox"/> Existing	<input checked="" type="checkbox"/> To be used without any modification <input type="checkbox"/> To be modified
	<input type="checkbox"/> New	<input type="checkbox"/> Standard equipment supplied by a manufacturer <input type="checkbox"/> CERN/collaboration responsible for the design and/or manufacturing
[insert lines if needed]		

HAZARDS GENERATED BY THE EXPERIMENT

(if using fixed installation) Hazards named in the document relevant for the fixed [COLLAPS, CRIS, ISOLTRAP, MINIBALL + only CD, MINIBALL + T-REX, NICOLE, SSP-GLM chamber, SSP-GHM chamber, or WITCH] installation.

Additional hazards:

<i>Hazards</i>		
	<i>Collection chamber and GLM beam line (SSP)</i>	<i>Mössbauer chamber at GLM beam line (SSP)</i>
Thermodynamic and fluidic		
Pressure		
Vacuum	typically, 10^{-6} mbar	typically, 10^{-6} mbar
Temperature	RT	RT – 800K
Heat transfer		

Thermal properties of materials			
Cryogenic fluid			
Electrical and electromagnetic			
Electricity		12 V, max. 5 A sample heating during measurements	
Static electricity			
Magnetic field	<input type="checkbox"/>		
Batteries	<input type="checkbox"/>		
Capacitors	<input type="checkbox"/>		
Ionizing radiation			
Target material		MnGa, MnAl, MnBi	
Beam particle type (e, p, ions, etc.)		ions	
Beam intensity		10^{11} ions/s	
Beam energy			
Cooling liquids	<input type="checkbox"/> [liquid]		
Gases	<input type="checkbox"/> [gas]		
Calibration sources:	<input type="checkbox"/>		
• Open source	<input type="checkbox"/>		
• Sealed source	<input type="checkbox"/> [ISO standard]		
• Isotope			
• Activity			
Use of activated material:			
• Description	<input type="checkbox"/> Collection in the chamber, removal from the chamber and transport to building 508	Measurement on-line with sample in the chamber	
• Dose rate on contact and in 10 cm distance		max. 0.5 Sv/h	
• Isotope		^{57}Mn and ^{119}In	
• Activity		max. 3-4 MBq per sample	
Non-ionizing radiation			
Laser			
UV light			
Microwaves (300MHz-30 GHz)			
Radiofrequency (1-300MHz)			
Chemical			
Toxic			
Harmful			
CMR (carcinogens, mutagens and substances toxic to reproduction)			
Corrosive			
Irritant			
Flammable			
Oxidizing			
Explosiveness			

Asphyxiant			
Dangerous for the environment			
Mechanical			
Physical impact or mechanical energy (moving parts)			
Mechanical properties (Sharp, rough, slippery)			
Vibration			
Vehicles and Means of Transport			
Noise			
Frequency			
Intensity			
Physical			
Confined spaces			
High workplaces			
Access to high workplaces			
Obstructions in passageways			
Manual handling			
Poor ergonomics			

0.1 Hazard identification

3.2 Average electrical power requirements (excluding fixed ISOLDE-installation mentioned above): *(make a rough estimate of the total power consumption of the additional equipment used in the experiment)*